Characterization of Nucleic Acid Higher Order Structure by Gas-Phase H/D Exchange in a Quadrupole-FT-ICR Mass Spectrometer

Jingjie Mo,* Gabrielle C. Todd, Kristina Håkansson
Department of Chemistry, University of Michigan, 930 North University Avenue, Ann Arbor, MI 48109-1055

Received 15 October 2008; revised 29 November 2008; accepted 15 December 2008
Published online 12 January 2009 in Wiley InterScience (www.interscience.wiley.com). DOI 10.1002/bip.21134

ABSTRACT:

Nucleic acid higher order structure is of intense interest in antisense and antigene strategies toward novel chemotherapeutic agents. Understanding how structural characteristics affect solution-phase properties is essential for a rational approach to nucleic acid-targeted drug design. The most dominant nucleic acid secondary structure is the hairpin, formed by intrastrand hydrogen bonding between complementary nucleobases. We have previously applied gas-phase hydrogen/deuterium exchange (HDX) with mass spectrometry detection to show that anionic DNA duplexes have lower HDX rates than their constituent monomers, indicating that hydrogen bonding can shield hydrogens from exchanging with the bath gas D_2S. The same HDX assay is applied here to investigate nucleic acid hairpin structure. Variations in hairpin solution-phase stabilities are achieved by changing their loop size, stem length, and stem composition (ratio of G/C and A/T(U) base pairs in the stem). These differences can be carried into the gas phase because electrospray ionization is a gentle ionization method that is able to preserve noncovalent interactions. Observed gas-phase HDX rates of these hairpins are consistent with their relative solution-phase stabilities as predicted by MFold, i.e., less stable nucleic acid hairpins exchange faster than more stable hairpins. To our knowledge, the presented experiments demonstrate for the first time that gas-phase HDX may be used to characterize nucleic acid higher order structure and the results suggest that the relative stabilities of nucleic acid hairpins in the gaseous phase are correlated with those in solution. © 2009 Wiley Periodicals, Inc. Biopolymers 91: 256–264, 2009.

Keywords: *nucleic acid structure; hydrogen exchange; mass spectrometry*

This article was originally published online as an accepted preprint. The "Published Online" date corresponds to the preprint version. You can request a copy of the preprint by emailing the Biopolymers editorial office at biopolymers@wiley.com

INTRODUCTION

Biomolecules fold into characteristic secondary and tertiary structures that account for their diverse functional activities. For example, the three-dimensional configuration of an RNA molecule determines many of its biological properties, including its involvement in gene expression, regulatory processes, mRNA splicing, transport, and translation.[1–7] It is well established that single-stranded nucleic acid molecules possess the capability of condensing into compact structures by virtue of intrastrand interaction to form secondary structures.[8,9] This type of interaction has been well characterized by X-ray crystallography,[10–12] NMR spectroscopy,[13,14] fluorescence resonance energy transfer techniques,[15] as well as relatively indirect approaches such as enzymatic digestion,[16–20] chemical

Present address: GlaxoSmithKline, 709 Swedeland Road, King of Prussia, PA 19406.
Correspondence to: Kristina Håkansson; e-mail: kicki@umich.edu
Contract grant sponsor: Petroleum Research Fund
Contract grant sponsor: Thermo Electron (American Society for Mass Spectrometry)
Contract grant sponsor: NSF CAREER Award
Contract grant number: CHE-05-47699

probing,[17,18,21] electrophoresis,[22,23] and phylogenetic conservation.[24,25]

With the development of soft ionization methods, e.g., matrix-assisted laser desorption/ionization[26,27] and electrospray ionization (ESI),[28,29] which, in some cases, are able to retain memory of solution-phase structure when molecules are transferred into the gas phase, the use of mass spectrometry (MS) for structural analysis of biological molecules has become increasingly routine. Common mass spectrometric approaches for characterizing nucleic acid structure include ion mobility analysis,[30] and the use of MS in conjunction with solution-phase chemical footprinting.[31] Efficacy of these approaches is limited, however, as the first only provides information about the molecular cross section and the second strategy requires extensive sample manipulation before MS analysis. Our group has previously applied tandem mass spectrometry (MS^n) to differentiate three isomeric DNA 15-mers, two of which are predicted to form hairpin structures in solution and the third without a preferred solution-phase conformation.[32] Results from electron detachment dissociation (EDD)/infrared multiphoton dissociation MS^3 and activated ion EDD in which precursor ions were briefly heated with an IR laser before EDD suggested a correlation between gas- and solution-phase structures for these 15-mers and provided some information on their relative stabilities as the more stable structure generated fewer product ions than the less stable ones. However, this approach is limited to relatively small molecules because of the low fragmentation efficiency of EDD.

Gas-phase hydrogen exchange (HDX),[33–37] in which exchange rate constants are much smaller than those in solution (solution-phase exchange occurs on a millisecond time scale because of the high opening rate of Watson-Crick base pairs) has been proposed as an alternative method for structural analysis of nucleic acids.[36,38–44] Combining HDX with MS is a practical way to investigate gas-phase structures of biomolecules as well as their differences from solution-phase structures.[33–37,40] We have recently shown that gas-phase HDX in the external collision cell of a hybrid quadrupole-Fourier transform ion cyclotron resonance (FT-ICR) mass spectrometer may be a useful technique for characterization of nucleic acid higher order structure because nucleic acid duplexes displayed lower HDX rates than their constituent monomers, due to hydrogens participating in base pairing being protected from exchange.[45] Specifically, the monomers d(GCATGC) and d(TGGGGT) exchanged ~80% of their heteroatom bound hydrogens (including both backbone and nucleobase hydrogens) in 50 s whereas their corresponding Watson-Crick and Hoogsteen duplexes exchanged only ~40% (also including both backbone and nucleobase hydrogens) of their heteroatom bound hydrogens in the same time period.[45] In this work, we systematically investigate HDX of nucleic acid hairpins of varying stem length, loop size, and stem composition in an effort to seek a correlation between their solution-phase stabilities and gas-phase HDX rates.

MATERIALS AND METHODS

DNA (gel purified) and RNA (HPLC purified) were purchased from Yale Keck Facility (New Haven, CT) and Integrated DNA Technologies (Coralville, IA), respectively. Sequences of all the nucleic acids used are as follows (X = T for DNA and U for RNA) and their MFold[46,47] predicted structures (the MFold algorithm predicts a minimum free energy, ΔG, as well as minimum free energies for foldings that must contain any particular base pair[47]) are shown in Chart 1: 15-mer 1: CXAXCACXGAXAGGX, 15-mer 2: CXAX CACXGGAXAGX, 15-mer 3: CCGCCACXGGGCGGX, 15-mer 4: XAAXAACXGXAXXAX, 19-mer 2: CACACXGACXGCAGXGXGX, 19-mer 3, CGCGCCGACXGCGGCGCGX, 19-mer 4: CAXAXX GACXGCAAXAXGX. DNAs were used without further purification whereas RNAs were desalted by ethanol precipitation (protocol modified from Limbach et al.[48]: 1/3 volume of 10*M* NH_4OAc (pH = 7) and 2.5 volume of 100% cold ethanol were added to the RNA aqueous solution, samples were vortexed and stored at −80°C for 3 h, centrifuged for 15 min, and the supernatant was decanted. Then, 400 μL of cold 70% ethanol was added to the precipitate, samples were stored at −80°C for 2 h, centrifuged for 15 min, the supernatant was decanted, the precipitate was dried down, and dissolved in electrospray solution). Gas-phase deprotonated precursor ions were generated by negative ion mode ESI at 50 μL/h through an external Apollo II source equipped with dual ion funnels (Bruker Daltonics, Billerica, MA) in a spray solution consisting of 25% (vol/vol) methanol (Fisher, Fair Lawn, NJ) and 50 m*M* NH_4OAc (Fisher). Ion source transfer conditions, including the ion funnel DC voltages and skimmer voltages, were adjusted to be as "soft" as possible (higher charge states, which are not as stable as lower charge states, are observed under "soft" conditions) to maximally preserve nucleic acid higher order structure in the solution-to-gas phase transition. Analyte concentrations varied between 10 and 100 μM to get a signal-to-noise ratio of 10 in 8 scans.

All mass spectra were collected with an actively shielded 7 Tesla FT-ICR mass spectrometer (Bruker Daltonics) with a quadrupole front end (APEX-Q, Bruker Daltonics) as previously described.[32,49] This instrument comprises a focusing hexapole followed by a quadrupole mass filter which, in turn, is followed by a hexapole collision cell. Precursor ions in either 4^- or 5^- charge states were selected by the quadrupole and accumulated externally in the collision cell for 0.5 s, in the presence of D_2S (Cambridge Isotope Laboratories, Andover, MA) at a pressure of $\sim 5 \times 10^{-6}$ mbar (gauge factory calibrated for nitrogen, no further calibration was done). Multiple ICR cell fills were not used to avoid generation of mixtures of ion populations with different exposure time to D_2S (there is residual D_2S outside the storage hexapole). Gas-phase HDX reactions were performed for 0.51 to 30.5 s and mass spectra indicating mass shifts at each time point were recorded by XMASS (version 6.1 Bruker Daltonics). Data were processed with the MIDAS analysis software.[50]

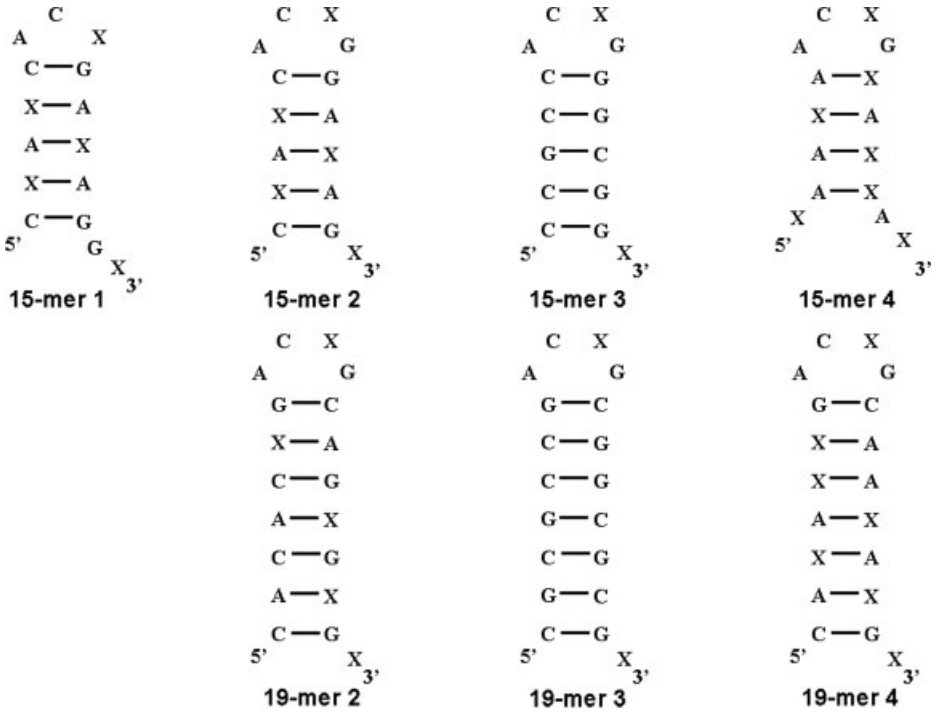

CHART 1 Nucleic acid structures predicted by Mfold Web Server[47] in solution (X = T for DNA and U for RNA). DNA/RNA 15-mer 1 has the same base composition as DNA/RNA 15-mer 2 but their sequences differ, resulting in a three-nucleotide-loop hairpin structure for 15mer-1 and a four-nucleotide loop for 15-mer 2. All the other nucleic acids characterized in this study have the preferable four-nucleotide-loop hairpin structure. DNA/RNA 15- and 19-mer 2 represent the mixed base pair stem hairpins; DNA/RNA 15- and 19-mer 3 represent the G/C rich hairpins, and DNA/RNA 15- and 19-mer 4 represent the A/T(U) rich hairpins. All the 19-mers have two more G/C base pairs in the hairpin stem than their corresponding 15-mers.

Percentage of HDX was calculated based on the average m/z of the entire oligonucleotide isotopic distribution, i.e., by considering the relative abundance of each isotopic peak, according to the following equation (adapted from Zhang and Smith[51])

$$\% \text{ deuterium incorporation} = [(m/z)_{\text{obs.}} - (m/z)_0]/[(m/z)_{\text{max.}} - (m/z)_0] \times 100\%$$

in which $(m/z)_{\text{obs.}}$ = observed average m/z following a particular exchange time, $(m/z)_0$ = average m/z prior to HDX, and $(m/z)_{\text{max.}}$ = expected average m/z at full deuteration of all exchangeable (i.e., heteroatom bound) hydrogens. Error bars (higher errors are expected with more deuterium incorporated) were generated from three individual experiments acquired on the same day due to difficulties with reproducing the D_2S pressure in the collision cell and the *t*-test was used for statistical analysis. Because of the fact that deuterium incorporation of nucleic acids reaches saturation after a short time period, typically within 1 min, data were only collected for the first 30 s to decrease sample consumption and to save time.

RESULTS AND DISCUSSION

Effects of Salt and Organic Solvent in Spray Solution on Gas-Phase HDX

Metal salts are known to play an important role in nucleic acid folding because they can shield negative charges on the backbone phosphate groups and thereby eliminate increased repulsive forces arising from compact secondary and tertiary structures. All nucleic acids investigated in this work are predicted to have a hairpin structure by the Mfold web server[46,47] in 1*M* Na^+ aqueous solution. However, such high Na^+ concentration in nucleic acid samples results in low negative mode ionization efficiency and low precursor ion abundance due to the distribution of signal among multiple Na^+-bound adducts. To overcome this limitation, NH_4^+ ions from ammonium acetate (NH_4OAc) instead of Na^+ have been used in previous studies. Ammonium ions neutralize backbone negative charges but can be stripped off from precursor

Table I Number of Exchangeable (i.e., Heteroatom Bound) Hydrogens for the 4^- and 5^- Charge States of Nucleic Acid Hairpins

	15-mer 1 (4^-)	15-mer 1 (5^-)	15-mer 2 (4^-)	15-mer 2 (5^-)	15-mer 3 (4^-)	15-mer 3 (5^-)	15-mer 4 (4^-)	15-mer 4 (5^-)	19-mer 2 (4^-)	19-mer 2 (5^-)	19-mer 3 (4^-)	19-mer 3 (5^-)	19-mer 4 (4^-)	19-mer 4 (5^-)
DNA	40	39	40	39	46	45	36	35	54	53	60	59	50	49
RNA	55	54	55	54	61	60	51	50	73	72	79	78	69	68

ions during ESI. For example, Gabelica and De Pauw[52] used 50 m*M* NH_4OAc for characterizing DNA duplexes and showed that DNA double helices were conserved. They also showed that with similar solvent (100 m*M* NH_4OAc) the structure of complexes between DNA duplexes and minor groove binders were preserved.[53] The effect of different cations in our experiment was investigated by comparing the gas-phase HDX rates of DNA hairpins electrosprayed from a solution containing 1 m*M* sodium acetate (NaOAc) to those electrosprayed from a solution containing 50 m*M* NH_4OAc. Statistically similar HDX rates were obtained for both DNA 15-mer 1 and DNA 15-mer 2 (see Chart 1 for structures and Table I for the number of exchangeable hydrogens) in these two different spray solutions, indicating similar effects of 1 m*M* Na^+ and 50 m*M* NH_4^+ on the gas-phase stabilities of nucleic acid hairpins (see Figure 1). This small influence from different types of counter ions is probably due to the enhanced hydrogen bonding in the gas phase resulting from the removal of polar solvent.[54–58] Gabelica and coworkers[52,53] have shown that thermal denaturation curves of DNA duplexes as well as their complexes with minor groove binders in the gas phase are similar to those in solution phase. Higher Na^+ concentrations were not tested due to the difficulty of generating precursor ions of acceptable signal-to-noise ratios. Instead, NH_4OAc was varied from 25 to 500 m*M* to investigate the concentration influence. Our results show statistically similar behavior for DNA 15-mer 2 at all concentrations (except at 25 m*M*, where slightly faster HDX rate was observed, Figure 2). Thus, 50 m*M* NH_4OAc was arbitrarily used for all following experiments.

Organic solvent in the spray solution greatly facilitates high ionization efficiency because it assists the extraction of precursor ions from ESI droplets by decreasing surface tension.[59,60] Although the presence of organic solvent may shift the folding equilibrium of nucleic acid hairpins in solution, when transferred into the gas phase, as mentioned earlier, the hydrogen bonds between base pairs should be enhanced due to the hydrophobic environment following removal of polar solvent.[54–58] Thus, we hypothesize the hairpin structure

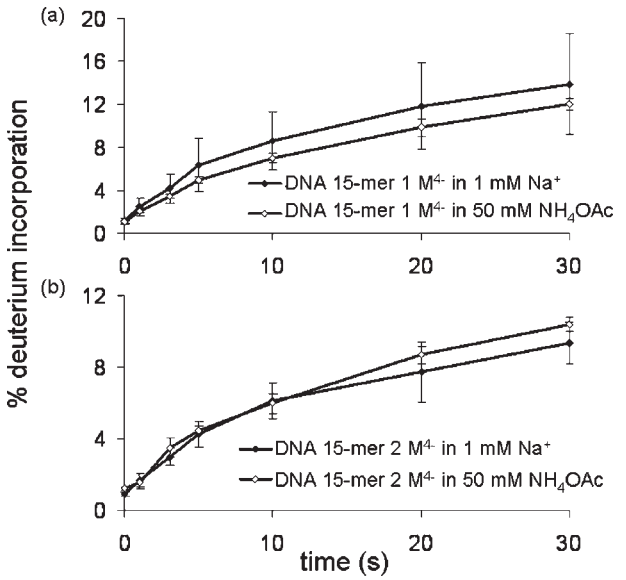

FIGURE 1 Gas-phase HDX of DNA 15-mer 1 (a) and 15-mer 2 (b) in 25% methanol and 1 m*M* Na^+ compared to those in 25% methanol and 50 m*M* NH_4OAc. Statistically similar results were observed for both DNAs in the two different spray solutions, indicating that 50 m*M* NH_4OAc has similar effect on nucleic acid stability as 1 m*M* Na^+.

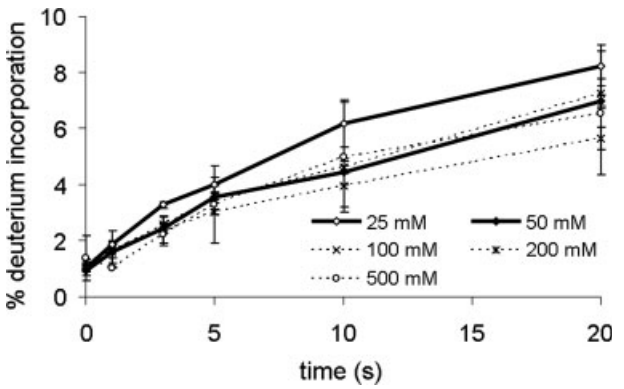

FIGURE 2 Gas-phase HDX of DNA 15-mer 2 electrosprayed at varying NH_4OAc concentrations. At 25 m*M* NH_4OAc (lowest concentration), the hairpin exchanges slightly faster than at higher concentrations. However, at 50 m*M* and above, there is no apparent influence of NH_4OAc concentration on the HDX rate. All further experiments were acquired at 50 m*M* NH_4OAc.

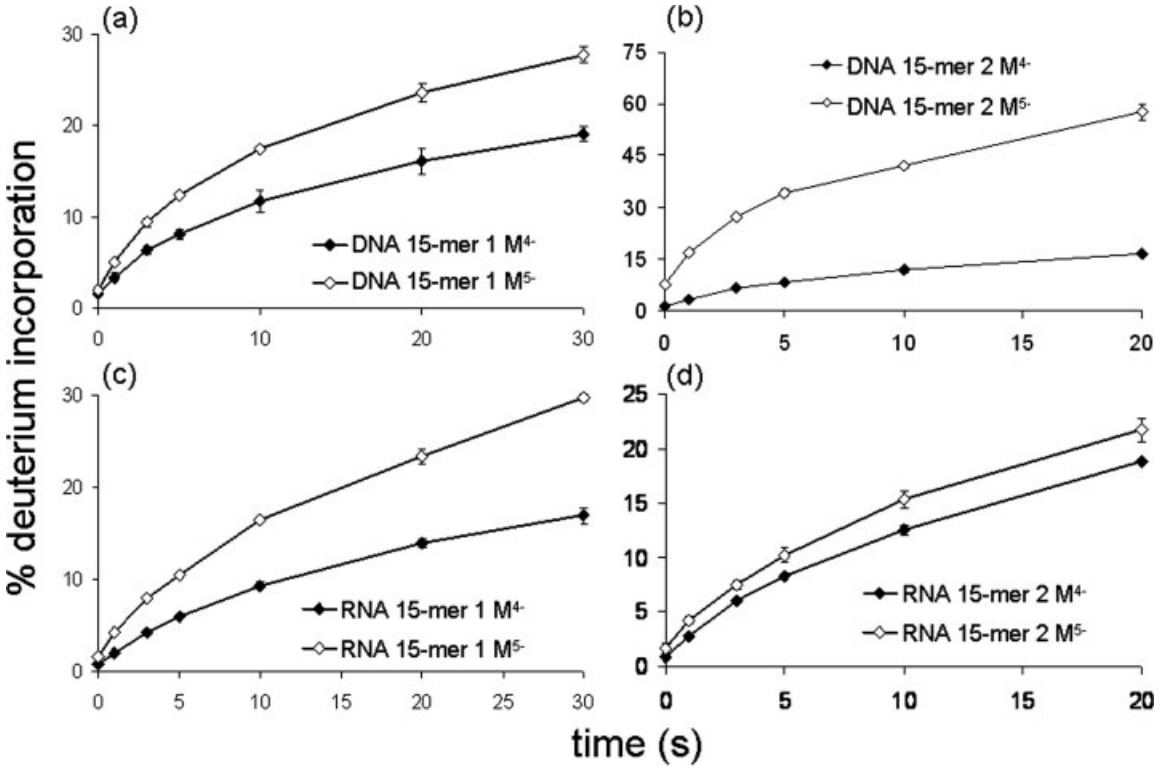

FIGURE 3 Gas-phase HDX of nucleic acid hairpins at different charge states. For all four nucleic acid hairpins (DNA 15-mer 1 (a), DNA 15-mer 2 (b), RNA 15-mer 1 (c), and RNA 15-mer 2 (d)), higher charge state (5^-) exchanges faster than lower charge state (4^-) of the same molecule, consistent with a more unfolded hairpin structure at higher charge state.

would still be favored in the gas phase. Nevertheless, the influence of organic solvent in the spray solution was investigated by comparing the gas-phase HDX rates of DNA 15-mer 2 in spray solutions with varying methanol percentages (5 to 95% with 5% increments). Results suggested that HDX behavior changed slightly at different methanol percentage but no clear trend was observed (data not shown). Therefore, 25% methanol was used for all subsequent experiments to eliminate the variable effects of organic solvents on HDX (20% methanol was used in the work discussed earlier by Gabelica and coworkers[52,53]).

Effect of Charge State on Gas-Phase HDX

ESI characteristically produces ions with multiple charge states,[28,29] which would influence the biomolecular higher order structure because Coulomb repulsion increases with increasing number of charge sites in the molecule, thereby presenting more unfolded structures,[61–70] and rendering hydrogens more accessible to HDX. Gas-phase HDX experiments were used to estimate the stabilities of nucleic acid higher order structures at different charge states. Figure 3 shows the comparison of gas-phase HDX rates of both DNA (a, b) and RNA (c, d) hairpins 15-mer 1 and 2 at their 4^- and 5^- charge states. In all four cases, the 5^- charge state exchanged faster than the 4^- charge state of the same molecule, consistent with the fact that biomolecules at higher charge states are less structured. Thus, the lowest possible charge state should be used for HDX experiments, a strategy that was adopted for all experiments presented below.

Effect of Hairpin Loop Size on Gas-Phase HDX

DNA/RNA 15-mers 1 and 2 have the same base composition but different sequences, resulting in a three-nucleotide and a four-nucleotide loop hairpin, respectively (Chart 1). The stability of the former hairpin is predicted to be lower than the stability of the latter by MFold (see ΔG values in Table II) and by thermal denaturation experiments.[71] Figure 4 displays gas-phase HDX of their 4^- charge state precursor ions. Deuterium incorporation in 15-mer 1 increases faster than that of 15-mer 2 for both DNA (Figure 4a, 30% vs. 20% in 20 s) and RNA (Figure 4b, 30% vs. 22% in 30s), indicating that the three-nucleotide loop hairpin is less stable than the four-

Table II **ΔG Values (in kcal/mol, Calculated by Mfold Web Server[47]) of Nucleic Acid Hairpins in Aqueous Solution of 1*M* Na^+**

	15-mer 1	15-mer 2	15-mer 3	15-mer 4	19-mer 2	19-mer 3	19-mer 4
DNA	−1.0	−1.8	−5.8	−0.6	−6.2	−10.5	−3.9
RNA	−2.5	−3.3	−8.8	+0.6	−9.1	−13.6	−4.9

More negative values represent more stable structures.

nucleotide-loop hairpin, consistent with the literature. The ratio of average deuterium incorporation into 15-mer 1 with respect to 15-mer 2 at each data point was 1.8 ± 0.2 for DNA and 1.5 ± 0.2 for RNA. When comparing these values to the ratio of MFold-predicted Δ*G* values for 15-mer 2 and 15-mer 1 (1.8 for DNA and 1.3 for RNA) in solution, they are numerically close, indicating that relative gas-phase HDX rates can reflect the relative solution-phase stability of nucleic acid hairpins with different loop sizes.

Effect of Hairpin Stem Length on Gas-Phase HDX

Another factor that influences hairpin stability is its stem length; longer stems have more base pairs and should therefore be more stable and less susceptible to HDX. Six pairs of nucleic acid hairpins (one 15-mer and one 19-mer) were selected for investigating the effect of stability for different stem lengths on gas-phase HDX behavior (structures are shown in Chart 1). The MFold predicted Δ*G* values of all six 19-mer hairpins (Table II) predict that they are more stable than their corresponding 15-mer hairpins because of the additional two G/C base pairs in the stem. When comparing the same charge states (5^-) of 19-mers and 15-mers, the relative exchange rates for both DNA and RNA correlate well with their relative solution-phase stabilities (see Figure 5). However, when comparing species of the same charge density (5^- charge state of 19-mer vs. 4^- charge state of 15-mer), the results are not consistent with their relative solution-phase stabilities and no conclusive trend could be found (data not shown). Therefore, we conclude that gas-phase HDX is able to demonstrate relative stabilities of nucleic acid hairpins with different stem lengths of the same charge state but not of the same charge density.

Effect of Hairpin Stem Composition on Gas-Phase HDX

The last factor of hairpin stability investigated was stem composition. Because of the fact that a G/C base pair has one more hydrogen bond than an A/T(U) base pair, slower HDX behavior is expected for hairpins with G/C rich stems compared to those with A/T(U) rich or mixed base pair stems. To characterize this effect, gas-phase HDX experiments were performed on DNA/RNA 15- and 19-mers 2, 3, and 4 (see Chart 1 for structures), which represent hairpins with mixed base pairs, G/C rich, and A/T(U) rich stems, respectively. The expected order of stabilities for these three groups is 3 > 2 > 4, and therefore the expected order of HDX rates is 3 < 2 < 4. Results are shown in Figure 6. In all cases, the mixed base pair stem hairpins exchange faster than their corresponding G/C rich hairpins, except for DNA 15-mers (Figure 6a) where these two groups exchange at similar rates, which is probably due to the relatively small difference in their Δ*G* values. A/T(U) rich hairpins always exchange faster than the other two hairpin types for DNAs as expected. For RNAs, however, they exchange faster than the G/C rich hairpins and slower than the mixed base pair stem hairpins. This

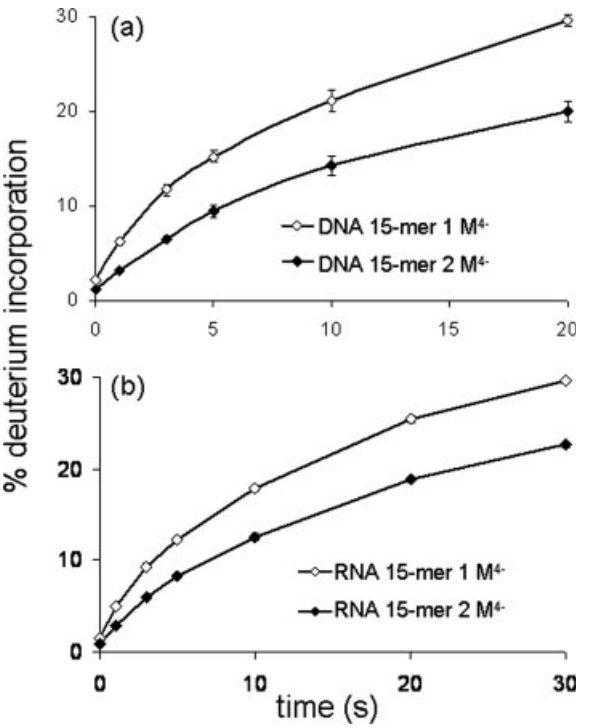

FIGURE 4 Gas-phase HDX of nucleic acid hairpins with a three-nucleotide loop compared to those with a four-nucleotide loop. The former undergoes exchange faster than the latter for both DNA (X = T) and RNA (X = U), consistent with their solution-phase stabilities as predicted by MFold.

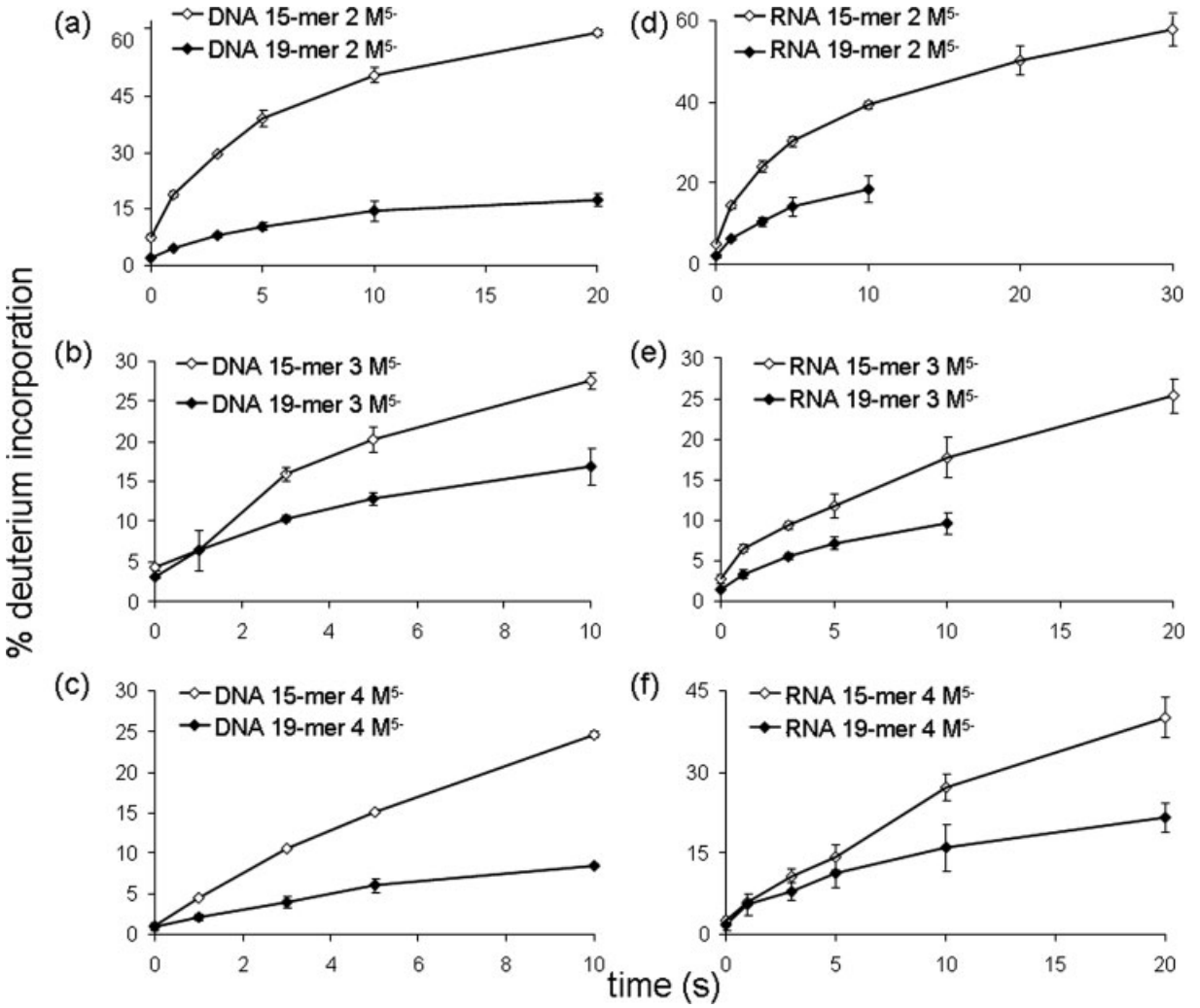

FIGURE 5 Gas-phase HDX of nucleic acid hairpins with different stem lengths. All of the three 19-mers contain two more G/C base pairs in the stem than their corresponding 15-mers, and, consequently, exchange slower than the 15-mers, which correlates with their predicted solution-phase stabilities.

unexpected behavior may be due to alternative gas-phase conformations of RNA A/U rich hairpins. For example, Mfold predicted a positive ΔG value for A/U rich RNA 15-mer 4, indicating hairpin formation is unfavorable in solution, thus difficult to compare its behavior with other hairpin structures. Overall, for nucleic acids capable of forming stable hairpin structures, their gas-phase HDX rates could be correlated to their relative solution-phase stabilities.

CONCLUSIONS

In this work, we show that gas-phase HDX combined with MS is a useful technique for characterization of nucleic acid higher order structure. The stability of hairpins, which are the dominant secondary structure of nucleic acids, depends on the loop size, stem length, and stem composition. Results from gas-phase HDX experiments of a set of nucleic acid hairpins suggest that their relative solution-phase stabilities can be reflected by their gas-phase HDX rates, i.e., more stable hairpins exchange slower than the less stable ones. For example, four-nucleotide-loop hairpins exchange slower than isomeric three-nucleotide-loop hairpins and G/C rich hairpins exchange slower than mixed stem hairpins, which exchange slower than A/T(U) rich hairpins (if they could form stable hairpin structure). The influence of salts in spray solution on nucleic acid higher order structure was also investigated and NH_4^+ was found to have similar effect for neutralizing the backbone negative charges as Na^+ and its concentration does not appear to have significant influence on HDX rates. However, organic solvent was found to have

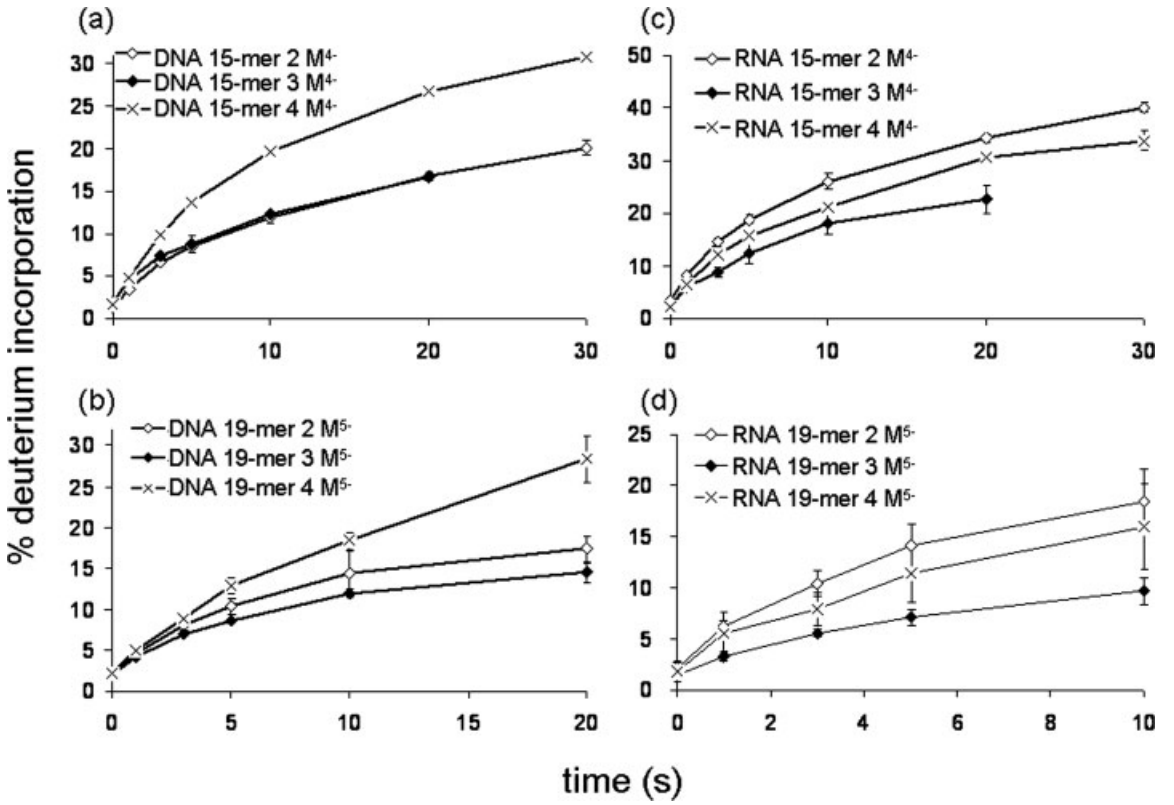

FIGURE 6 Gas-phase HDX of nucleic acid hairpins with different stem compositions (percentage of G/C base pairs in the stem). For correlation with ΔG values, HDX rates should follow the trend DNA/RNA 4 > DNA/RNA 2 > DNA/RNA 3. However, observed rates for RNA 15- and 19-mer 4 deviate from this behavior, possibly because they have too many A/T base pairs in the stem such that formation of a hairpin is not favorable. Instead, they may fold into other structures in the gas phase.

some influence on the gas-phase HDX rates but the trend is not clear. Overall, the presented gas-phase HDX experiments suggest that HDX levels are consistent with the relative structural stabilities of nucleic acid hairpins in solution.

REFERENCES

1. Adams, C. C.; Stern, D. B. Nucleic Acids Res 1990, 18, 6003–6010.
2. Gesteland, R. F.; Cech, T. R.; Atkins, J. F. The RNA World; Cold Spring Harbor Laboratory Press: New York, 1999.
3. Gottlieb, E. Proc Natl Acad Sci USA 1992, 89, 7164–7168.
4. Klausner, R.; Rouault, T.; Harford, J. Cell 1993, 72, 19–28.
5. Skripkin, E.; Paillart, J. C.; Marquet, R.; Ehresmann, B.; Ehresmann, C. Proc Natl Acad Sci USA 1994, 91, 4945–4949.
6. Tuerk, C.; Gauss, P.; Thermes, C.; Groebe, D. R.; Gayles, M.; Guild, N.; Stormo, G.; d'Aubenton-Carafa, Y; Uhlenbeck, O. C.; Tinoco, I.; Brody, E. N.; Gold, L. Proc Natl Acad Sci USA 1988, 85, 1364–1368.
7. Yang, S. L.; Temin, H. M. EMBO J 1994, 13, 713–726.
8. James, J.; Tinoco, I. J Nucleic Acids Res 1993, 21, 3287–3293.
9. Panayotatos, N.; Wells, R. Nature 1981, 289, 466–470.
10. Ban, N.; Nissen, P.; Hansen, J.; Moore, P. B.; Steitz, T. A. Science 2000, 289, 905–920.
11. Wimberly, B. T.; Brodersen, D. E.; Clemons, W. M. J.; Morgan-Warren, R. J.; Carter, A. P.; Vonrhein, C.; Hartsch, T.; Ramakrishnan, V. Nature 2000, 407, 327–329.
12. Carter, A. P.; Celmons, W. M.; Brodersen, D. E.; Morgan-Warren, R. J.; Wimberly, B. T.; Ramakrishnam, V. Nature 2000, 407, 340–348.
13. Al-Hashimi, H. M. ChemBioChem 2005, 6, 1472–1473.
14. Latham, M. P.; Brown, D. J.; McCallum, S. A.; Pardi, A. ChemBioChem 2005, 6, 1492–1505.
15. Klostermeier, D.; Millar, D. P. Methods 2001, 23, 240–254.
16. Noller, H. F.; Woese, C. R. Science 1981, 212, 403–411.
17. Ehresmann, C.; Baudin, F.; Mougel, M.; Romby, P.; Ebel, J.; Ehresmann, B. Nucleic Acids Res 1987, 15, 9109–9127.
18. Parker, R. Methods Enzymol 1989, 180, 510–517.
19. Pavlakis, G. N.; Lockard, R. E.; Vamvakopoulos, N.; Lauren Rieser, L.; Rajbhandary, U. L.; Vournakis, J. N. Cell 1980, 19, 91–102.
20. Yao, Y.; Wang, Q.; Hao, Y.; Tan, Z. Nucleic Acids Res 2007, 35, e68.
21. Peattie, D. A.; Gilbert, W. Proc Natl Acad Sci USA 1980, 77, 4679–4682.

22. Ross, A.; Brimacombe, R. Nature 1979, 281, 271–276.
23. Glotz, C.; Zwieb, C.; Brimacombe, R.; Edwards, K.; Kossel, H. Nucleic Acids Res 1981, 9, 3287–3306.
24. Gutell, R. R.; Gray, M. W.; Schnare, M. N. Nucleic Acids Res 1993, 21, 3055–3074.
25. Woese, C. R.; Pace, H. R. The RNA World; Cold Spring Harbor: New York, 1993.
26. Tanaka, K.; Waki, H.; Ido, Y.; Akita, S.; Yoshida, Y.; Yoshida, T. Rapid Commun Mass Spectrom 1988, 2, 151–153.
27. Karas, M.; Hillenkamp, F. Anal Chem 1988, 60, 2299–2301.
28. Fenn, J. B.; Mann, M.; Meng, C. K.; Wong, S. F.; Whitehouse, C. M. Science 1989, 246, 64–71.
29. Fenn, J. B.; Mann, M.; Meng, C. K.; Wong, S. F. Mass Spectrom Rev 1990, 9, 37–70.
30. Gidden, J.; Baker, E. S.; Ferzoco, A.; Bowers, M. T. Int J Mass Spectrom 2005, 240, 183–193.
31. Yu, E.; Fabris, D. J Mol Biol 2003, 330, 211–223.
32. Mo, J.; Hakansson, K. Anal Bioanal Chem 2006, 386, 675–681.
33. Freitas, M. A.; Hendrickson, C. L.; Emmett, M. R.; Marshall, A. G. J Am Soc Mass Spectrom 1998, 9, 1012–1019.
34. Campbell, S.; Rodgers, M. T.; Marzluff, E. M.; Beauchamp, J. L. J Am Chem Soc 1994, 116, 9765.
35. Gard, E.; Green, M. K.; Bregar, J.; Lebrilla, C. B. J Am Soc Mass Spectrom 1994, 5, 623–631.
36. Green, M. K.; Lebrilla, C. B. Mass Spectrom Rev 1997, 16, 53–71.
37. Wyttenbach, T.; Bowers, M. T. J Am Soc Mass Spectrom 1999, 10, 9–14.
38. Chipuk, J. E.; Brodbelt, J. S. J Am Soc Mass Spectrom 2007, 18, 724–736.
39. Crestoni, M. E.; Fornarini, S. J Mass Spectrom 2003, 38, 854–861.
40. Robinson, J. M.; Greig, M. J.; Griffey, R. H.; Mohan, V.; Laude, D. A. Anal Chem 1998, 70, 3566–3571.
41. Griffey, R. H.; Greig, M. J.; Robinson, J. M.; Laude, D. A. Rapid Commun Mass Spectrom 1999, 13, 113–117.
42. Hofstadler, S. A.; Sannes-Lowery, K. A.; Griffey, R. H. J Mass Spectrom 2000, 35, 62–70.
43. Gabelica, V.; Rosu, F.; Witt, M.; Baykut, G.; de Pauw, E. Rapid Commun Mass Spectrom 2005, 19, 201–208.
44. Freitas, M. A.; Marshall, A. G. J Am Soc Mass Spectrom 2001, 12, 780–785.
45. Mo, J. J.; Hakansson, K. Anal Chem 2007, 79, 7893–7898.
46. Mathews, D. H.; Sabina, J.; Zuker, M.; Turner, D. H. J Mol Biol 1999, 288, 911–940.
47. Zuker, M. Nucleic Acids Res 2003, 31, 3406–3415.
48. Limbach, P. A.; Crain, P. F.; McCloskey, J. M. J Am Soc Mass Spectrom 1995, 6, 27–39.
49. Yang, J.; Mo, J.; Adamson, J. T.; Hakansson, K. Anal Chem 2005, 77, 1876–1882.
50. Senko, M. W.; Canterbury, J. D.; Guan, S.; Marshall, A. G. Rapid Commun Mass Spectrom 1996, 10, 1839–1844.
51. Zhang, Z.; Smith, D. L. Protein Sci 1993, 2, 522–531.
52. Gabelica, V.; De Pauw, E. Int J Mass Spectrom 2002, 219, 151–159.
53. Gabelica, V.; Rosu, F.; Houssier, C.; De Pauw, E. Rapid Commun Mass Spectrom 2000, 14, 464–467.
54. Thomas, R. K. Proc R Soc A 1971, 322, 137–146.
55. Gao, J.; Carbeck, J. Q.; Smith, R. D.; Whitesides, G. M. Biophys J 1999, 76, 3253–3260.
56. Gao, Q. Y.; Cheng, X. H.; Smith, R. D.; Yang, C. F.; Goldberg, I. H. J Mass Spectrom 1996, 31, 31–36.
57. Rogniaux, H.; Van Dorsselaer, A.; Barth, P.; Biellmann, J. F.; Barbanton, J.; van Zandt, M.; Chevrier, B.; Howard, E.; Mitschler, A.; Potier, N.; Urzhumtseva, L.; Moras, D.; Podjarny, A. J Am Soc Mass Spectrom 1999, 10, 635–647.
58. Saenger, W. Principles of Nucleic Acid Structure; Springer-Verlag: New York, 1984.
59. Ikonomou, M. G.; Blades, A. T.; Kebarle, P. Anal Chem 1991, 63, 1989–1998.
60. Tang, L.; Kebarle, P. Anal Chem 1991, 63, 2709–2715.
61. Chowdhury, S. K.; Katta, V.; Chait, B. T. J Am Chem Soc 1990, 112, 9013–9015.
62. Loo, J. A.; Edmonds, C. G.; Udseth, H. R.; Smith, R. D. Anal Chem 1990, 62, 693–698.
63. Mirza, U. A.; Cohen, S. L.; Chait, B. T. Anal Chem 1993, 65, 1–6.
64. Wagner, D. S.; Anderegg, R. J. Anal Chem 1994, 66, 706–711.
65. Konermann, L.; Collings, B. A.; Douglas, D. J. Biochemistry 1997, 36, 5554–5559.
66. Konermann, L.; Rosell, F. I.; Mauk, A. G.; Douglas, D. J. Biochemistry 1997, 36, 6448–6454.
67. Konermann, L.; Douglas, D. J. Biochemistry 1997, 36, 12296–12302.
68. Konermann, L.; Douglas, D. J. Rapid Commun Mass Spectrom 1998, 12, 435–442.
69. Konermann, L.; Douglas, D. J. J Am Soc Mass Spectrom 1998, 9, 1248–1254.
70. Vincent, W. S.; Lee, V. W. S.; Chen, Y. L.; Konermann, L. Anal Chem 1999, 71, 4154.
71. Groebe, D. R.; Uhlenbeck, O. C. Nucleic Acids Res 1988, 16, 11725–11735.

Reviewing Editor: Dan Fabris